An introduction to Hybrid High-Order methods with application to incompressible fluid mechanics

Daniele A. Di Pietro

Institut Montpelliérain Alexander Grothendieck, University of Montpellier

SISSA, 7 March 2019

Features

- Capability of handling general polyhedral meshes
- Construction valid for arbitrary space dimensions
- Arbitrary approximation order (including $k = 0$)
- Robustness with respect to the variations of the physical coefficients
- Reduced computational cost after static condensation

Outline

Outline

Polyhedral meshes

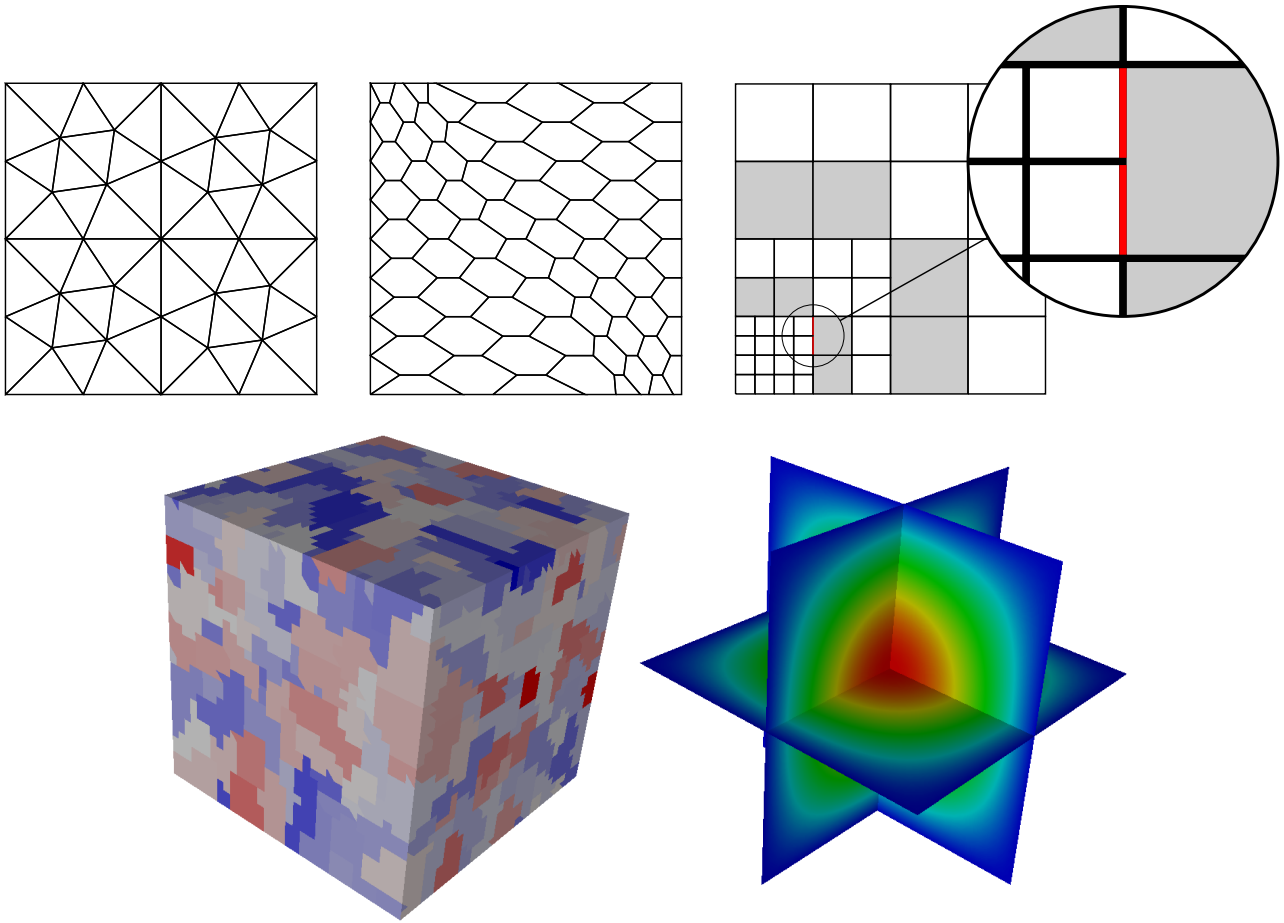

Figure: Supported meshes in 2d and 3d, and HHO solution on the agglomerated 3d mesh. For the notions of polytopal mesh and regular polytopal mesh sequence see [DP and Tittarelli, 2018]

Model problem

- Let $\Omega \subset \mathbb{R}^d$, $d \geq 1$, denote a bounded, connected polyhedral domain
- For $f \in L^2(\Omega)$, we consider the Poisson problem

$$\begin{aligned} -\Delta u &= f && \text{in } \Omega \\ u &= 0 && \text{on } \partial\Omega \end{aligned}$$

- Denote by $(\cdot,\cdot)_X$ the $L^2(X)$-inner product ($X = \Omega$ omitted)
- In weak form: Find $u \in H^1_0(\Omega)$ s.t.

$$a(u,v) := (\boldsymbol{\nabla} u, \boldsymbol{\nabla} v) = (f,v) \qquad \forall v \in H^1_0(\Omega)$$

Projectors on local polynomial spaces

- With $X = T$ or $X = F$, the L^2-projector $\pi_X^{0,l} : L^2(X) \longrightarrow \mathbb{P}^l(X)$ is s.t.

$$(\pi_X^{0,l} v - v, w)_X = 0 \text{ for all } w \in \mathbb{P}^l(X)$$

- The elliptic projector $\pi_T^{1,l} : H^1(T) \longrightarrow \mathbb{P}^l(T)$ is s.t.

$$(\boldsymbol{\nabla}(\pi_T^{1,l} v - v), \boldsymbol{\nabla} w)_T = 0 \text{ for all } w \in \mathbb{P}^l(T) \text{ and } \int_T (\pi_T^{1,l} v - v) = 0$$

- Both have optimal approximation properties in $\mathbb{P}^l(T)$
- See [DP and Droniou, 2017a, DP and Droniou, 2017b]

Computing $\pi_T^{1,k+1}$ from L^2-projections of degree k

- Recall the following IBP valid for all $v \in H^1(T)$ and all $w \in C^\infty(\overline{T})$:

$$\boxed{(\boldsymbol{\nabla} v, \boldsymbol{\nabla} w)_T = -(v, \Delta w)_T + \sum_{F \in \mathcal{F}_T} (v, \boldsymbol{\nabla} w \cdot \boldsymbol{n}_{TF})_F}$$

- Specializing it to $w \in \mathbb{P}^{k+1}(T)$, we can write

$$(\boldsymbol{\nabla} \pi_T^{1,k+1} v, \boldsymbol{\nabla} w)_T = -(\pi_T^{0,k} v, \Delta w)_T + \sum_{F \in \mathcal{F}_T} (\pi_F^{0,k} v, \boldsymbol{\nabla} w \cdot \boldsymbol{n}_{TF})_F$$

- Moreover, it can be easily seen that

$$\int_T (\pi_T^{1,k+1} v - v) = \int_T (\pi_T^{1,k+1} v - \pi_T^{0,k} v) = 0$$

- **Hence, $\pi_T^{1,k+1} v$ can be computed from $\pi_T^{0,k} v$ and $(\pi_F^{0,k} v)_{F \in \mathcal{F}_T}$!**

Discrete unknowns

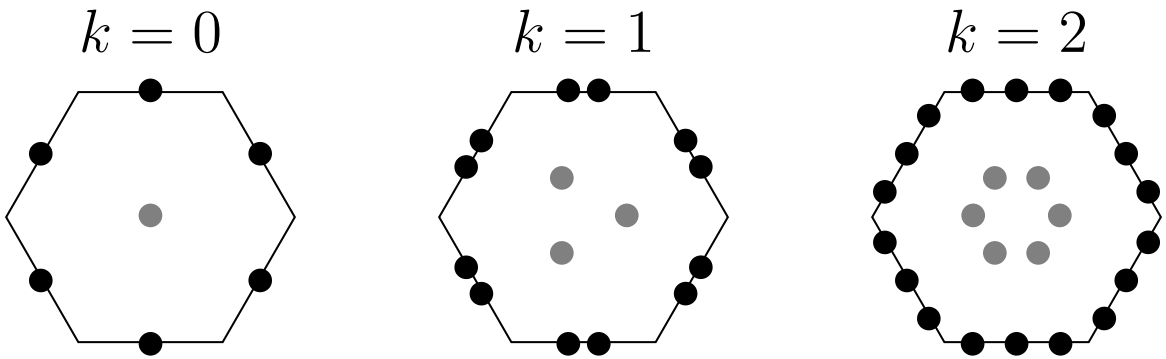

Figure: $\underline{U}_T^k$ for $k \in \{0, 1, 2\}$

- Let a polynomial degree $k \geq 0$ be fixed
- For all $T \in \mathcal{T}_h$, we define the local space of discrete unknowns

$$\underline{U}_T^k := \left\{ \underline{v}_T = (v_T, (v_F)_{F \in \mathcal{F}_T}) \ : \ v_T \in \mathbb{P}^k(T) \text{ and } v_F \in \mathbb{P}^k(F) \quad \forall F \in \mathcal{F}_T \right\}$$

- The local interpolator $\underline{I}_T^k : H^1(T) \to \underline{U}_T^k$ is s.t., for all $v \in H^1(T)$,

$$\underline{I}_T^k v := \left(\pi_T^{0,k} v, (\pi_F^{0,k} v)_{F \in \mathcal{F}_T} \right)$$

Local potential reconstruction

- Let $T \in \mathcal{T}_h$. We define the local potential reconstruction operator

$$r_T^{k+1} : \underline{U}_T^k \to \mathbb{P}^{k+1}(T)$$

s.t., for all $\underline{v}_T \in \underline{U}_T^k$, $\int_T (r_T^{k+1}\underline{v}_T - v_T) = 0$ and

$$\boxed{(\boldsymbol{\nabla} r_T^{k+1}\underline{v}_T, \boldsymbol{\nabla} w)_T = -(v_T, \Delta w)_T + \sum_{F \in \mathcal{F}_T} (v_F, \boldsymbol{\nabla} w \cdot \boldsymbol{n}_{TF})_F \quad \forall w \in \mathbb{P}^{k+1}(T)}$$

- By construction, we have

$$\boxed{r_T^{k+1} \circ \underline{I}_T^k = \pi_T^{1,k+1}}$$

- $r_T^{k+1} \circ \underline{I}_T^k$ has therefore optimal approximation properties in $\mathbb{P}^{k+1}(T)$

Stabilization I

- We would be tempted to approximate

$$a_{|T}(u,v) \approx (\boldsymbol{\nabla} r_T^{k+1} \underline{u}_T, \boldsymbol{\nabla} r_T^{k+1} \underline{v}_T)_T$$

- This choice, however, is not stable in general. We consider instead

$$\boxed{\mathrm{a}_T(\underline{u}_T, \underline{v}_T) \coloneqq (\boldsymbol{\nabla} r_T^{k+1} \underline{u}_T, \boldsymbol{\nabla} r_T^{k+1} \underline{v}_T)_T + \mathrm{s}_T(\underline{u}_T, \underline{v}_T)}$$

- The role of s_T is to ensure $\|\cdot\|_{1,T}$-coercivity with

$$\|\underline{v}_T\|_{1,T}^2 \coloneqq \|\boldsymbol{\nabla} v_T\|_T^2 + \sum_{F \in \mathcal{F}_T} \frac{1}{h_F} \|v_F - v_T\|_F^2 \quad \forall \underline{v}_T \in \underline{U}_T^k$$

Stabilization II

Assumption (Stabilization bilinear form)

The bilinear form $\mathrm{s}_T : \underline{U}_T^k \times \underline{U}_T^k \to \mathbb{R}$ satisfies the following properties:

- Symmetry and positivity. s_T is symmetric and positive semidefinite.
- Stability. It holds, with hidden constant independent of h and T,

$$\mathrm{a}_T(\underline{v}_T, \underline{v}_T)^{\frac{1}{2}} \simeq \|\underline{v}_T\|_{1,T} \quad \forall \underline{v}_T \in \underline{U}_T^k.$$

- Polynomial consistency. For all $w \in \mathbb{P}^{k+1}(T)$ and all $\underline{v}_T \in \underline{U}_T^k$,

$$\mathrm{s}_T(\underline{I}_T^k w, \underline{v}_T) = 0.$$

Stabilization III

- The following stable choice violates polynomial consistency:

$$\mathrm{s}_T^{\mathrm{hdg}}(\underline{u}_T, \underline{v}_T) \coloneqq \sum_{F \in \mathcal{F}_T} h_F^{-1}(u_F - u_T, v_F - v_T)_F$$

- To circumvent this problem, we penalize the high-order differences

$$(\delta_T^k \underline{v}_T, (\delta_{TF}^k \underline{v}_T)_{F \in \mathcal{F}_T}) \coloneqq \underline{I}_T^k r_T^{k+1} \underline{v}_T - \underline{v}_T$$

- The classical HHO stabilization bilinear form reads

$$\boxed{\mathrm{s}_T(\underline{u}_T, \underline{v}_T) \coloneqq \sum_{F \in \mathcal{F}_T} h_F^{-1} \left((\delta_T^k - \delta_{TF}^k)\underline{u}_T, (\delta_T^k - \delta_{TF}^k)\underline{v}_T \right)_F}$$

Discrete problem

- Define the global space with single-valued interface unknowns

$$\underline{U}_h^k := \Big\{ \underline{v}_h = ((v_T)_{T\in\mathcal{T}_h}, (v_F)_{F\in\mathcal{F}_h}) \ : \ v_T \in \mathbb{P}^k(T) \quad \forall T \in \mathcal{T}_h \text{ and } v_F \in \mathbb{P}^k(F) \quad \forall F \in \mathcal{F}_h \Big\}$$

  and its subspace with strongly enforced boundary conditions

$$\underline{U}_{h,0}^k := \{ \underline{v}_h \in \underline{U}_h^k \ : \ v_F = 0 \quad \forall F \in \mathcal{F}_h^{\mathrm{b}} \}$$

- The discrete problem reads: Find $\underline{u}_h \in \underline{U}_{h,0}^k$ s.t.

$$\boxed{\mathrm{a}_h(\underline{u}_h, \underline{v}_h) := \sum_{T\in\mathcal{T}_h} \mathrm{a}_T(\underline{u}_T, \underline{v}_T) = \sum_{T\in\mathcal{T}_h} (f, v_T)_T \quad \forall \underline{v}_h \in \underline{U}_{h,0}^k}$$

- Well-posedness follows from coercivity and discrete Poincaré

Convergence

Theorem (Energy-norm error estimate)

Assume $u \in H_0^1(\Omega) \cap H^{k+2}(\mathcal{T}_h)$. *The following energy error estimate holds:*

$$\boxed{\|\boldsymbol{\nabla}_h(r_h^{k+1}\underline{u}_h - u)\| + |\underline{u}_h|_{s,h} \lesssim h^{k+1}|u|_{H^{k+2}(\mathcal{T}_h)},}$$

with $(r_h^{k+1}\underline{u}_h)_{|T} := r_T^{k+1}\underline{u}_T$ *for all* $T \in \mathcal{T}_h$ *and* $|\underline{u}_h|_{s,h}^2 := \sum_{T\in\mathcal{T}_h} \mathrm{s}_T(\underline{u}_T, \underline{u}_T)$.

Theorem (Superclose L^2-norm error estimate)

Further assuming elliptic regularity and $f \in H^1(\mathcal{T}_h)$ *if* $k = 0$,

$$\boxed{\|r_h^{k+1}\underline{u}_h - u\| \lesssim h^{k+2}\mathcal{N}_k,}$$

with $\mathcal{N}_0 := \|f\|_{H^1(\mathcal{T}_h)}$ *and* $\mathcal{N}_k := |u|_{H^{k+2}(\mathcal{T}_h)}$ *for* $k \geq 1$.

Static condensation I

- Fix a basis for $\underline{U}_{h,0}^k$ with functions supported by only one T or F
- Partition the discrete unknowns into element- and interface-based:

$$\mathsf{U}_h = \begin{bmatrix} \mathsf{U}_{\mathcal{T}_h} \\ \mathsf{U}_{\mathcal{F}_h^{\mathrm{i}}} \end{bmatrix}$$

- U_h solves the following linear system:

$$\begin{bmatrix} \mathsf{A}_{\mathcal{T}_h\mathcal{T}_h} & \mathsf{A}_{\mathcal{T}_h\mathcal{F}_h^{\mathrm{i}}} \\ \mathsf{A}_{\mathcal{F}_h^{\mathrm{i}}\mathcal{T}_h} & \mathsf{A}_{\mathcal{F}_h^{\mathrm{i}}\mathcal{F}_h^{\mathrm{i}}} \end{bmatrix} \begin{bmatrix} \mathsf{U}_{\mathcal{T}_h} \\ \mathsf{U}_{\mathcal{F}_h^{\mathrm{i}}} \end{bmatrix} = \begin{bmatrix} \mathsf{F}_{\mathcal{T}_h} \\ 0 \end{bmatrix}$$

- $\mathsf{A}_{\mathcal{T}_h\mathcal{T}_h}$ **is block-diagonal and SPD, hence inexpensive to invert**

Static condensation II

- This remark suggests a two-step solution strategy:
  1. Element unknowns are eliminated solving the local balances

$$\mathsf{U}_{\mathcal{T}_h} = \mathsf{A}_{\mathcal{T}_h\mathcal{T}_h}^{-1}\left(\mathsf{F}_{\mathcal{T}_h} - \mathsf{A}_{\mathcal{T}_h\mathcal{F}_h^{\mathrm{i}}}\mathsf{U}_{\mathcal{F}_h^{\mathrm{i}}}\right)$$

  2. Face unknowns are obtained solving the global transmission problem

$$\mathsf{A}_h^{\mathrm{sc}}\mathsf{U}_{\mathcal{F}_h^{\mathrm{i}}} = -\mathsf{A}_{\mathcal{T}_h\mathcal{F}_h^{\mathrm{i}}}^{\mathrm{T}}\mathsf{A}_{\mathcal{T}_h\mathcal{T}_h}^{-1}\mathsf{F}_{\mathcal{T}_h}$$

     with global system matrix

$$\mathsf{A}_h^{\mathrm{sc}} := \mathsf{A}_{\mathcal{F}_h^{\mathrm{i}}\mathcal{F}_h^{\mathrm{i}}} - \mathsf{A}_{\mathcal{T}_h\mathcal{F}_h^{\mathrm{i}}}^{\mathrm{T}}\mathsf{A}_{\mathcal{T}_h\mathcal{T}_h}^{-1}\mathsf{A}_{\mathcal{T}_h\mathcal{F}_h^{\mathrm{i}}}$$

- $\mathsf{A}_h^{\mathrm{sc}}$ **is SPD and its stencil involves neighbours through faces**

Numerical examples

2d test case, smooth solution, uniform refinement

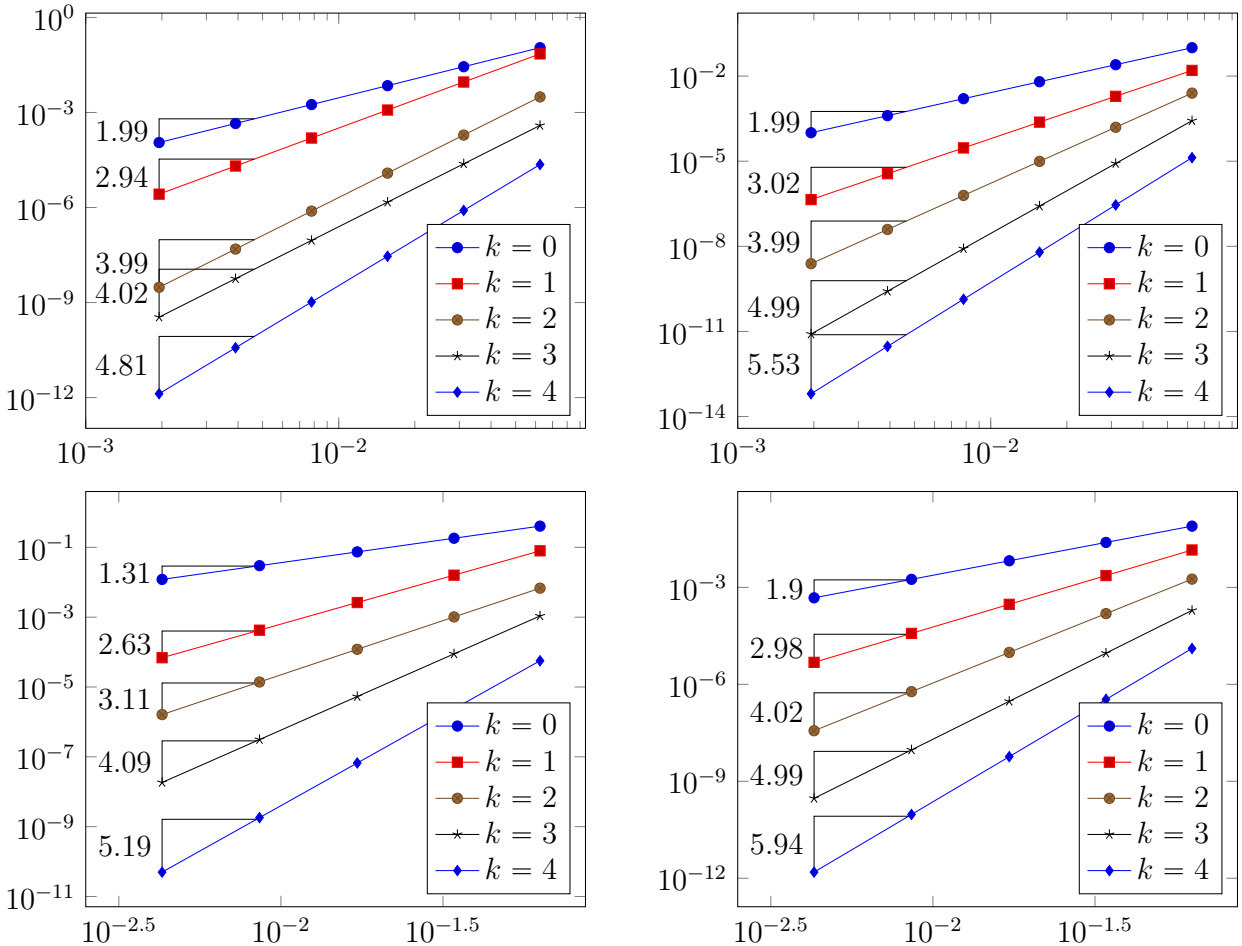

Figure: 2d test case, trigonometric solution. Energy (left) and L^2-norm (right) of the error vs. h for uniformly refined triangular (top) and hexagonal (bottom) mesh families

Numerical examples I

3d industrial test case, adaptive refinement, cost assessment

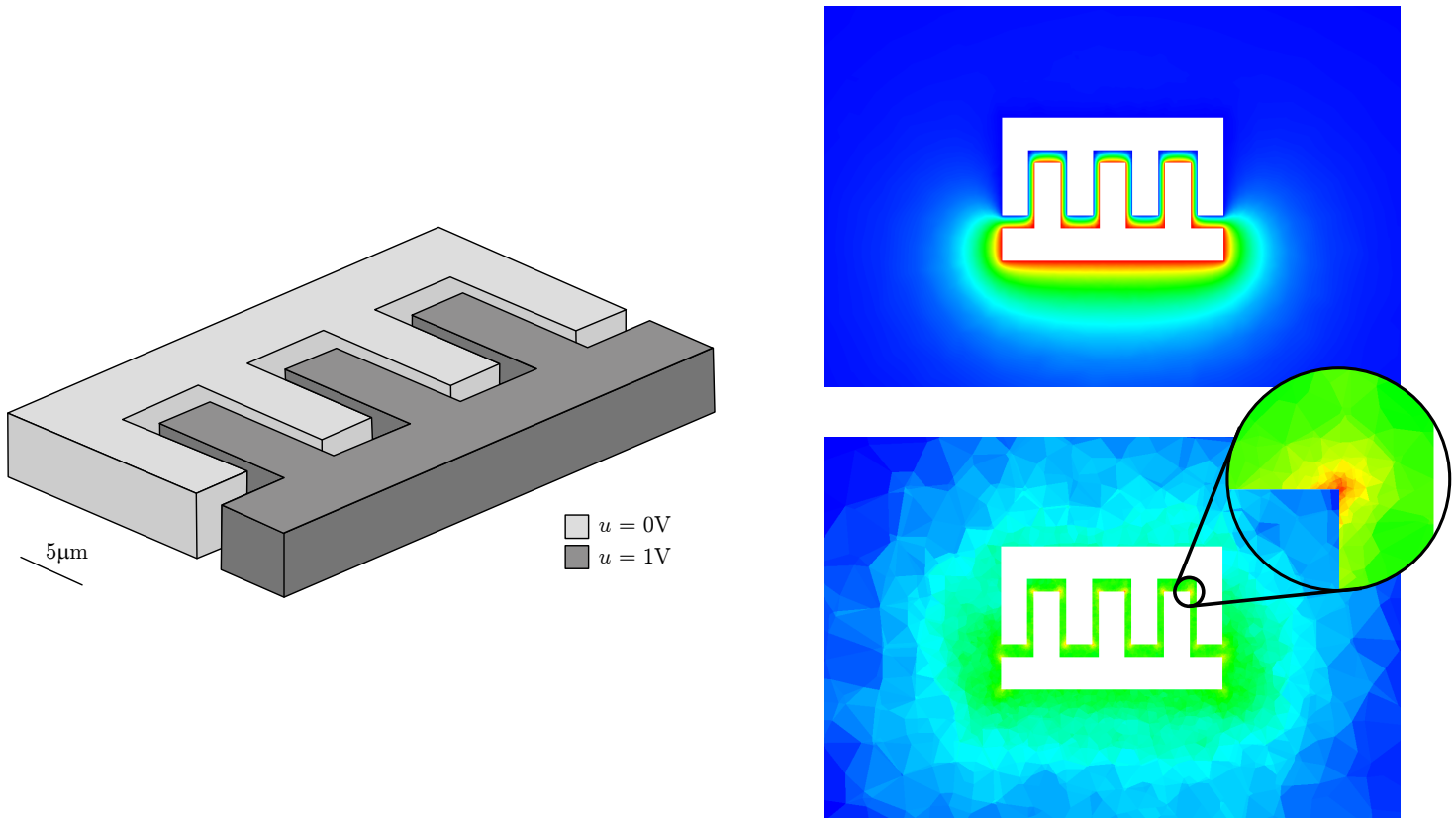

Figure: Geometry (left), numerical solution (right, top) and final adaptive mesh (right, bottom) for the comb-drive actuator test case [DP and Specogna, 2016]

Numerical examples II

3d industrial test case, adaptive refinement, cost assessment

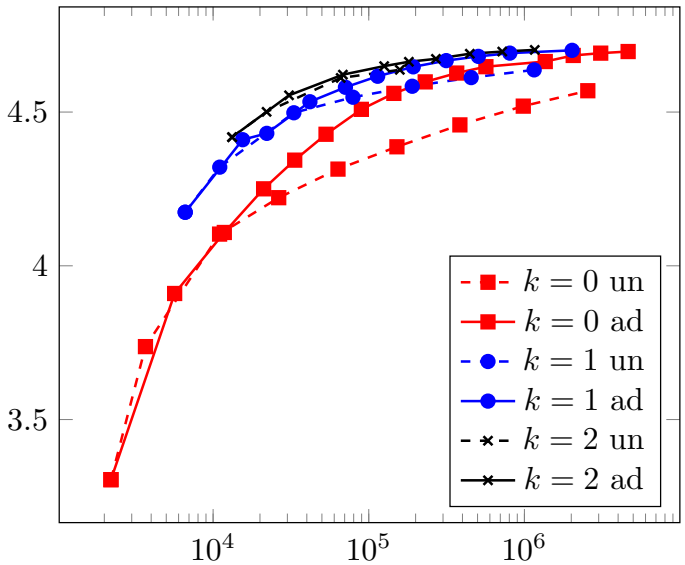

(a) Capacitance vs. $N_{\mathrm{dof},\boldsymbol{h}}$

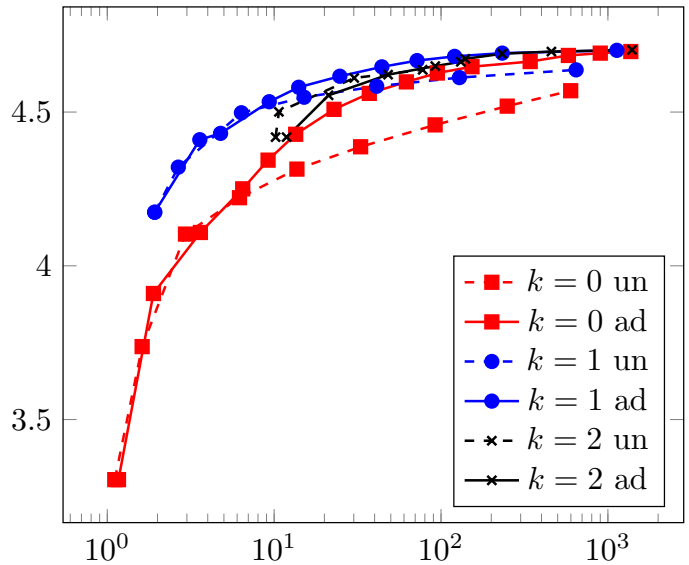

(b) Capacitance vs. computing time

Figure: Results for the comb drive benchmark.

Numerical examples III

3d industrial test case, adaptive refinement, cost assessment

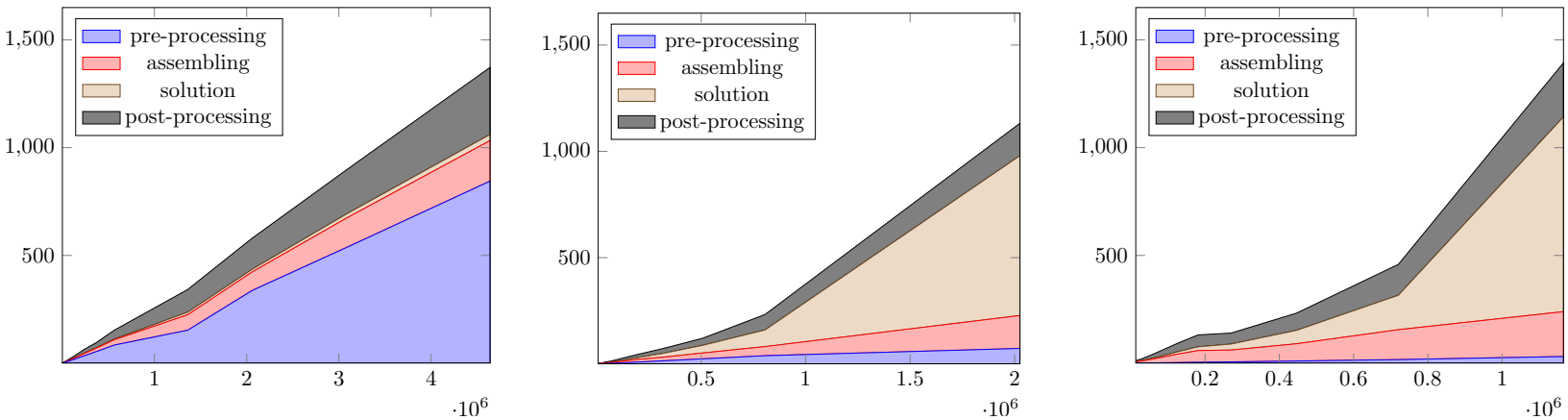

(a) $k = 0$ (b) $k = 1$ (c) $k = 2$

Figure: Computing wall time (s) vs. number of DOFs for the comb drive benchmark, AGMG solver.

Numerical examples I

3d test case, singular solution, adaptive coarsening

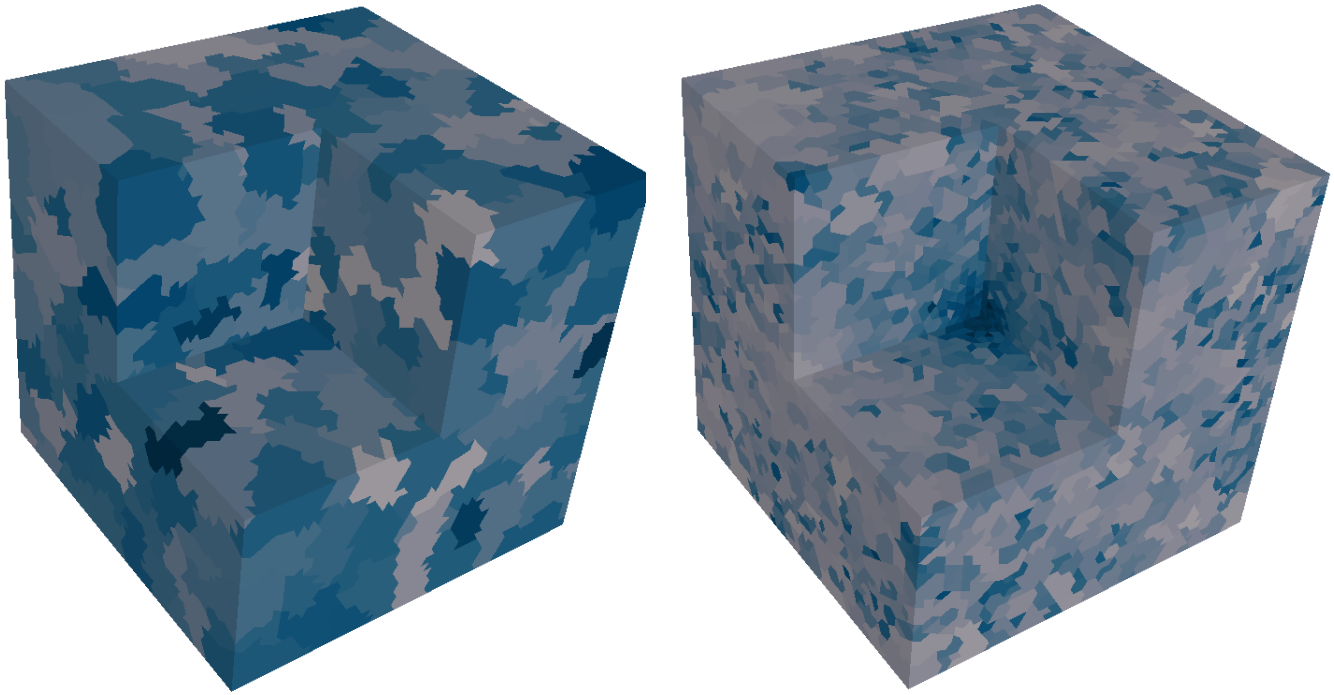

Figure: Fichera corner benchmark, adaptive mesh coarsening [DP and Specogna, 2016]

Numerical examples II

3d test case, singular solution, adaptive coarsening

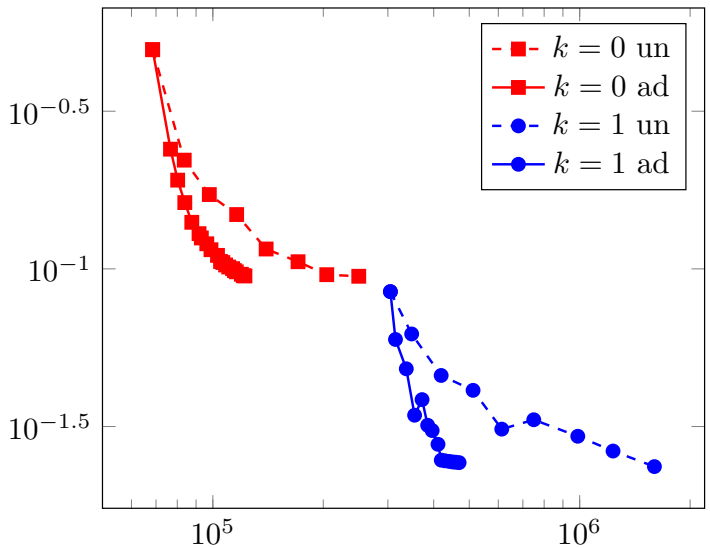

(a) Energy-error vs. N_{dofs}

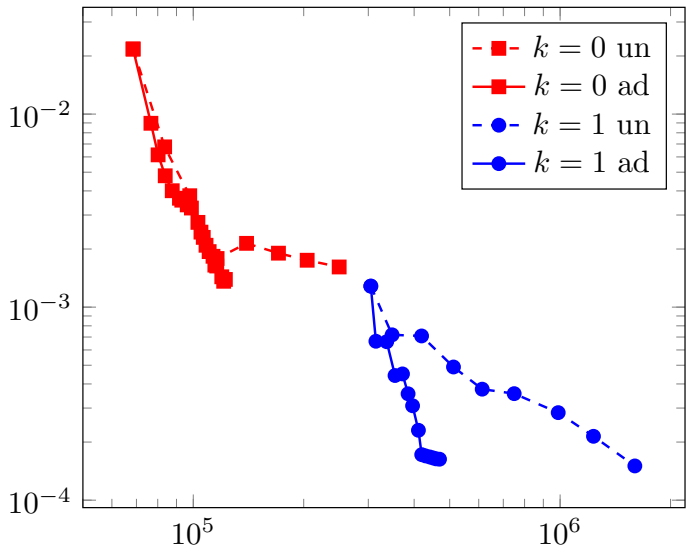

(b) L^2-error vs. N_{ndof}

Figure: Error vs. number of DOFs for the Fichera corner benchmark, adaptively coarsened meshes

Outline

Features

- Capability of handling general polyhedral meshes
- Construction valid for both $d = 2$ and $d = 3$
- Arbitrary approximation order (including $k = 0$)
- Inf-sup stability on general meshes
- Robust handling of dominant advection
- Local conservation of momentum and mass
- Reduced computational cost after static condensation

$$N_{\mathrm{dof},h} = d\,\mathrm{card}(\mathcal{F}_h^{\mathrm{i}})\binom{k+d-1}{d-1} + \mathrm{card}(\mathcal{T}_h)$$

HHO for incompressible flows

- MHO for Stokes [Aghili, Boyaval, DP, 2015]
- Pressure-robust HHO for Stokes [DP, Ern, Linke, Schieweck, 2016]
- Péclet-robust HHO for Oseen [Aghili and DP, 2018]
- Darcy-robust HHO for Brinkman [Botti, DP, Droniou, 2018]
- Skew-symmetric HHO for Navier–Stokes [DP and Krell, 2018]
- Temam's device for HHO [Botti, DP, Droniou, 2018]

The incompressible Navier–Stokes equations I

- Let $d \in \{2,3\}$, $\nu \in \mathbb{R}_+^*$, $\boldsymbol{f} \in L^2(\Omega)^d$, $\boldsymbol{U} \coloneqq H_0^1(\Omega)^d$, and $P \coloneqq L_0^2(\Omega)$
- The INS problem reads: Find $(\boldsymbol{u}, p) \in \boldsymbol{U} \times P$ s.t.

$$\boxed{\begin{aligned} \nu a(\boldsymbol{u},\boldsymbol{v}) + t(\boldsymbol{u},\boldsymbol{u},\boldsymbol{v}) + b(\boldsymbol{v},p) &= \int_\Omega \boldsymbol{f}\cdot\boldsymbol{v} \qquad && \forall \boldsymbol{v} \in \boldsymbol{U}, \\ -b(\boldsymbol{u},q) &= 0 && \forall q \in L^2(\Omega), \end{aligned}}$$

with viscous and pressure-velocity coupling bilinear forms

$$a(\boldsymbol{w},\boldsymbol{v}) \coloneqq \int_\Omega \boldsymbol{\nabla}\boldsymbol{w} : \boldsymbol{\nabla}\boldsymbol{v}, \quad b(\boldsymbol{v},q) \coloneqq -\int_\Omega q\boldsymbol{\nabla}\cdot\boldsymbol{v}$$

and convective trilinear form

$$t(\boldsymbol{w},\boldsymbol{v},\boldsymbol{z}) \coloneqq \int_\Omega (\boldsymbol{w}\cdot\boldsymbol{\nabla})\boldsymbol{v}\cdot\boldsymbol{z} = \sum_{i=1}^d \sum_{j=1}^d \int_\Omega w_j(\partial_j v_i) z_i$$

Discrete spaces I

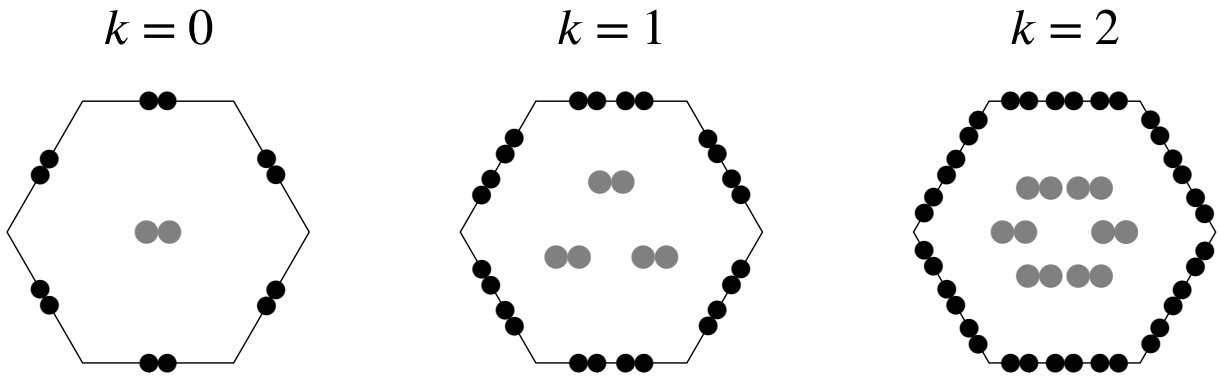

Figure: Local velocity space $\underline{\boldsymbol{U}}_T^k$ for $k \in \{0, 1, 2\}$

- For $k \geq 0$, we define the global space of discrete velocity unknowns

$$\underline{\boldsymbol{U}}_h^k := \Big\{ \underline{\boldsymbol{v}}_h = ((\boldsymbol{v}_T)_{T\in\mathcal{T}_h}, (\boldsymbol{v}_F)_{F\in\mathcal{F}_h}) \ : \ \boldsymbol{v}_T \in \mathbb{P}^k(T)^d \quad \forall T \in \mathcal{T}_h \text{ and } \boldsymbol{v}_F \in \mathbb{P}^k(F)^d \quad \forall F \in \mathcal{F}_h \Big\}$$

- The restrictions to $T \in \mathcal{T}_h$ are $\underline{\boldsymbol{U}}_T^k$ and $\underline{\boldsymbol{v}}_T = (\boldsymbol{v}_T, (\boldsymbol{v}_F)_{F\in\mathcal{F}_T})$

Discrete spaces II

- The global interpolator $\underline{\boldsymbol{I}}_h^k : H^1(\Omega)^d \to \underline{\boldsymbol{U}}_h^k$ is s.t., $\forall \boldsymbol{v} \in H^1(\Omega)^d$,

$$\underline{\boldsymbol{I}}_h^k \boldsymbol{v} := \left((\boldsymbol{\pi}_T^{0,k} \boldsymbol{v})_{T \in \mathcal{T}_h}, (\boldsymbol{\pi}_F^{0,k} \boldsymbol{v})_{F \in \mathcal{F}_h}\right)$$

- The velocity space strongly accounting for boundary conditions is

$$\underline{\boldsymbol{U}}_{h,0}^k := \left\{ \underline{\boldsymbol{v}}_h \in \underline{\boldsymbol{U}}_h^k \ : \ \boldsymbol{v}_F = \boldsymbol{0} \quad \forall F \in \mathcal{F}_h^{\mathrm{b}} \right\}$$

  equipped with the H_0^1-like norm $\|\cdot\|_{1,h}$

- The discrete pressure space is defined setting

$$P_h^k := \left\{ q_h \in \mathbb{P}^k(\mathcal{T}_h) \ : \ \int_\Omega q_h = 0 \right\} \subset P$$

Gradient, velocity, and divergence reconstructions I

- For $\ell \geq 0$, the gradient reconstruction $\boldsymbol{G}_T^\ell : \underline{\boldsymbol{U}}_T^k \to \mathbb{P}^\ell(T)^{d\times d}$ is s.t.

$$\int_T \boldsymbol{G}_T^\ell \underline{\boldsymbol{v}}_T : \boldsymbol{\tau} = -\int_T \boldsymbol{v}_T \cdot (\boldsymbol{\nabla}\cdot\boldsymbol{\tau}) + \sum_{F\in\mathcal{F}_T} \int_F \boldsymbol{v}_F \cdot (\boldsymbol{\tau}\, \boldsymbol{n}_{TF}) \quad \forall \boldsymbol{\tau} \in \mathbb{P}^\ell(T)^{d\times d}$$

- The divergence reconstruction $D_T^\ell : \underline{\boldsymbol{U}}_T^k \to \mathbb{P}^\ell(T)$ is s.t.

$$D_T^\ell \underline{\boldsymbol{v}}_T := \mathrm{tr}(\boldsymbol{G}_T^\ell \underline{\boldsymbol{v}}_T)$$

- The velocity reconstruction $\boldsymbol{r}_T^{k+1}$ is as for Poisson component-wise
- By construction, it holds

$$\boldsymbol{G}_T^k \circ \underline{\boldsymbol{I}}_T^k = \boldsymbol{\pi}_T^k, \qquad D_T^k \circ \underline{\boldsymbol{I}}_T^k = \pi_T^{0,k}, \qquad \boldsymbol{r}_T^{k+1} \circ \underline{\boldsymbol{I}}_T^k = \boldsymbol{\pi}_T^{1,k+1}$$

Viscous term

- The viscous term is discretized by means of the bilinear form a_h s.t.

$$\mathrm{a}_h(\underline{\boldsymbol{u}}_h, \underline{\boldsymbol{v}}_h) \coloneqq \sum_{T \in \mathcal{T}_h} \mathrm{a}_T(\underline{\boldsymbol{u}}_T, \underline{\boldsymbol{v}}_T)$$

  with local contribution

$$\boxed{\mathrm{a}_T(\underline{\boldsymbol{w}}_T, \underline{\boldsymbol{v}}_T) \coloneqq (\boldsymbol{\nabla} \boldsymbol{r}_T^{k+1} \underline{\boldsymbol{w}}_T, \boldsymbol{\nabla} \boldsymbol{r}_T^{k+1} \underline{\boldsymbol{v}}_T)_T + \mathrm{s}_T(\underline{\boldsymbol{w}}_T, \underline{\boldsymbol{v}}_T)}$$

- As in the scalar case, several possible choices for s_T ensure that

$$\mathrm{a}_h(\underline{\boldsymbol{v}}_h, \underline{\boldsymbol{v}}_h) \simeq \|\underline{\boldsymbol{v}}_h\|_{1,h}^2 \quad \forall \underline{\boldsymbol{v}}_h \in \underline{\boldsymbol{U}}_h^k$$

- Variable viscosity can be treated following [DP and Ern, 2015]

Pressure-velocity coupling

- The pressure-velocity coupling is realized by means of

$$\mathrm{b}_h(\underline{\boldsymbol{v}}_h, q_h) \coloneqq -\sum_{T\in\mathcal{T}_h}\int_T D_T^k\underline{\boldsymbol{v}}_T q_T$$

- Uniform inf-sup condition: There is $\beta > 0$ independent of h s.t.

$$\boxed{\forall q_h \in P_h^k,\quad \beta\|q_h\|_{L^2(\Omega)} \le \sup_{\underline{\boldsymbol{v}}_h\in\underline{\boldsymbol{U}}_{h,0}^k,\|\underline{\boldsymbol{v}}_h\|_{1,h}=1} \mathrm{b}_h(\underline{\boldsymbol{v}}_h, q_h)}$$

- This stability result is valid on general meshes and for any $k \ge 0$
- Use Fortin's trick after observing that, for all $\boldsymbol{v} \in H^1(T)^d$,

$$D_T^k\underline{\boldsymbol{I}}_T^k\boldsymbol{v} = \pi_T^{0,k}\boldsymbol{v} \text{ for all } T\in\mathcal{T}_h \text{ and } \|\underline{\boldsymbol{I}}_h^k\boldsymbol{v}\|_{1,h} \lesssim |\boldsymbol{v}|_{H^1(\Omega)^d}$$

Convective term: A key remark I

- We have the following IBP formula: For all $\boldsymbol{w}, \boldsymbol{v}, \boldsymbol{z} \in H^1(\Omega)^d$,

$$\boxed{\int_\Omega (\boldsymbol{w}\cdot\boldsymbol{\nabla})\boldsymbol{v}\cdot\boldsymbol{z} + \int_\Omega (\boldsymbol{w}\cdot\boldsymbol{\nabla})\boldsymbol{z}\cdot\boldsymbol{v} + \int_\Omega (\boldsymbol{\nabla}\cdot\boldsymbol{w})(\boldsymbol{v}\cdot\boldsymbol{z}) = \int_{\partial\Omega} (\boldsymbol{w}\cdot\boldsymbol{n})(\boldsymbol{v}\cdot\boldsymbol{z})}$$

- Using this formula with $\boldsymbol{w} = \boldsymbol{v} = \boldsymbol{z} = \boldsymbol{u}$, we get

$$t(\boldsymbol{u},\boldsymbol{u},\boldsymbol{u}) = \int_\Omega (\boldsymbol{u}\cdot\boldsymbol{\nabla})\boldsymbol{u}\cdot\boldsymbol{u} = -\frac{1}{2}\int_\Omega (\boldsymbol{\nabla}\cdot\boldsymbol{u})(\boldsymbol{u}\cdot\boldsymbol{u}) + \frac{1}{2}\int_{\partial\Omega} (\boldsymbol{u}\cdot\boldsymbol{n})(\boldsymbol{u}\cdot\boldsymbol{u}) = 0,$$

  where we have used the mass equation and the boundary condition

- **Reproducing this non-dissipation property is the key!**

Convective term: A key remark II

- The discrete velocity may not be divergence-free (and zero on $\partial\Omega$)
- We can used as a starting point modified versions of t:

$$t^{\mathrm{ss}}(\boldsymbol{w},\boldsymbol{v},\boldsymbol{z}) := \frac{1}{2}\int_\Omega (\boldsymbol{w}\cdot\boldsymbol{\nabla})\boldsymbol{v}\cdot\boldsymbol{z} - \frac{1}{2}\int_\Omega (\boldsymbol{w}\cdot\boldsymbol{\nabla})\boldsymbol{z}\cdot\boldsymbol{v}$$

or, following [Temam, 1979],

$$\boxed{t^{\mathrm{tm}}(\boldsymbol{w},\boldsymbol{v},\boldsymbol{z}) := \int_\Omega (\boldsymbol{w}\cdot\boldsymbol{\nabla})\boldsymbol{v}\cdot\boldsymbol{z} + \frac{1}{2}\int_\Omega (\boldsymbol{\nabla}\cdot\boldsymbol{w})(\boldsymbol{v}\cdot\boldsymbol{z}) - \frac{1}{2}\int_{\partial\Omega} (\boldsymbol{w}\cdot\boldsymbol{n})(\boldsymbol{v}\cdot\boldsymbol{z})}$$

- **t^{ss} and t^{tm} are non-dissipative even if $\boldsymbol{\nabla}\cdot\boldsymbol{w} \neq 0$ and $\boldsymbol{v}_{|\partial\Omega} \neq \boldsymbol{0}$**

Directional derivative reconstruction

- Let $\underline{\boldsymbol{w}}_T \in \underline{\boldsymbol{U}}_T^k$ represent a velocity field on T
- We let the directional derivative reconstruction

$$G_T^k(\underline{\boldsymbol{w}}_T;\cdot) : \underline{\boldsymbol{U}}_T^k \to \mathbb{P}^k(T)^d$$

be s.t., for all $\boldsymbol{z} \in \mathbb{P}^k(T)^d$,

$$\int_T G_T^k(\underline{\boldsymbol{w}}_T;\underline{\boldsymbol{v}}_T)\cdot\boldsymbol{z} = \int_T (\boldsymbol{w}_T\cdot\boldsymbol{\nabla})\boldsymbol{v}_T\cdot\boldsymbol{z} + \sum_{F\in\mathcal{F}_T}\int_F (\boldsymbol{w}_F\cdot\boldsymbol{n}_{TF})(\boldsymbol{v}_F-\boldsymbol{v}_T)\cdot\boldsymbol{z}$$

- $G_T^k(\underline{\boldsymbol{w}}_T;\underline{\boldsymbol{v}}_T)$ and $\boldsymbol{G}_T^{2k}\underline{\boldsymbol{v}}_T$ are linked: For all $\boldsymbol{z} \in \mathbb{P}^k(T)^d$,

$$\int_T G_T^k(\underline{\boldsymbol{w}}_T;\underline{\boldsymbol{v}}_T)\cdot\boldsymbol{z} = \int_T (\boldsymbol{w}_T\cdot\boldsymbol{G}_T^{2k})\underline{\boldsymbol{v}}_T\cdot\boldsymbol{z} + \sum_{F\in\mathcal{F}_T}\int_F (\boldsymbol{w}_F-\boldsymbol{w}_T)\cdot\boldsymbol{n}_{TF}(\boldsymbol{v}_F-\boldsymbol{v}_T)\cdot\boldsymbol{z}$$

Discrete global integration by parts formula

We reproduce at the discrete level the formula:

$$\int_\Omega (\boldsymbol{w}\cdot\boldsymbol{\nabla})\boldsymbol{v}\cdot\boldsymbol{z} + \int_\Omega (\boldsymbol{w}\cdot\boldsymbol{\nabla})\boldsymbol{z}\cdot\boldsymbol{v} + \int_\Omega (\boldsymbol{\nabla}\cdot\boldsymbol{w})(\boldsymbol{v}\cdot\boldsymbol{z}) = \int_{\partial\Omega} (\boldsymbol{w}\cdot\boldsymbol{n})(\boldsymbol{v}\cdot\boldsymbol{z})$$

Proposition (Discrete integration by parts formula)

It holds, for all $\underline{\boldsymbol{w}}_h, \underline{\boldsymbol{v}}_h, \underline{\boldsymbol{z}}_h \in \underline{\boldsymbol{U}}_h^k$,

$$\sum_{T\in\mathcal{T}_h} \int_T \left(G_T^k(\underline{\boldsymbol{w}}_T;\underline{\boldsymbol{v}}_T)\cdot\boldsymbol{z}_T + \boldsymbol{v}_T\cdot G_T^k(\underline{\boldsymbol{w}}_T;\underline{\boldsymbol{z}}_T) + D_T^{2k}\underline{\boldsymbol{w}}_T(\boldsymbol{v}_T\cdot\boldsymbol{z}_T)\right)$$

$$= \sum_{F\in\mathcal{F}_h^\flat} \int_F (\boldsymbol{w}_F\cdot\boldsymbol{n}_F)\boldsymbol{v}_F\cdot\boldsymbol{z}_F - \sum_{T\in\mathcal{T}_h}\sum_{F\in\mathcal{F}_T} \int_F (\boldsymbol{w}_F\cdot\boldsymbol{n}_{TF})(\boldsymbol{v}_F-\boldsymbol{v}_T)\cdot(\boldsymbol{z}_F-\boldsymbol{z}_T).$$

The term in red reflects the non-conformity of the method.

Convective term I

$$t^{\mathrm{tm}}(\boldsymbol{w},\boldsymbol{v},\boldsymbol{z}) \coloneqq \int_\Omega (\boldsymbol{w}\cdot\boldsymbol{\nabla})\boldsymbol{v}\cdot\boldsymbol{z} + \frac{1}{2}\int_\Omega (\boldsymbol{\nabla}\cdot\boldsymbol{w})(\boldsymbol{v}\cdot\boldsymbol{z}) \quad \forall \boldsymbol{w},\boldsymbol{v},\boldsymbol{z} \in \boldsymbol{U}$$

- Inspired by t^{tm}, we set

$$\mathrm{t}_h(\underline{\boldsymbol{w}}_h,\underline{\boldsymbol{v}}_h,\underline{\boldsymbol{z}}_h) \coloneqq \sum_{T\in\mathcal{T}_h} t_T(\underline{\boldsymbol{w}}_T,\underline{\boldsymbol{v}}_T,\underline{\boldsymbol{z}}_T)$$

  where, for all $T \in \mathcal{T}_h$,

$$\mathrm{t}_T(\underline{\boldsymbol{w}}_T,\underline{\boldsymbol{v}}_T,\underline{\boldsymbol{z}}_T) \coloneqq \int_T G_T^k(\underline{\boldsymbol{w}}_T;\underline{\boldsymbol{v}}_T)\cdot\boldsymbol{z}_T + \frac{1}{2}\int_T D_T^{2k}\underline{\boldsymbol{w}}_T(\boldsymbol{v}_T\cdot\boldsymbol{z}_T) + \frac{1}{2}\sum_{F\in\mathcal{F}_T}\int_F (\boldsymbol{w}_F\cdot\boldsymbol{n}_{TF})(\boldsymbol{v}_F-\boldsymbol{v}_T)\cdot(\boldsymbol{z}_F-\boldsymbol{z}_T)$$

- The second and third terms embody Temam's device

Discrete problem I

- The discrete problem reads: Find $(\underline{\boldsymbol{u}}_h, p_h) \in \underline{\boldsymbol{U}}_{h,0}^k \times P_h^k$ s.t.

$$\boxed{\begin{aligned} \nu \mathrm{a}_h(\underline{\boldsymbol{u}}_h, \underline{\boldsymbol{v}}_h) + \mathrm{t}_h(\underline{\boldsymbol{u}}_h, \underline{\boldsymbol{u}}_h, \underline{\boldsymbol{v}}_h) + \mathrm{b}_h(\underline{\boldsymbol{v}}_h, p_h) &= \int_\Omega \boldsymbol{f} \cdot \boldsymbol{v}_h \quad && \forall \underline{\boldsymbol{v}}_h \in \underline{\boldsymbol{U}}_{h,0}^k, \\ -\mathrm{b}_h(\underline{\boldsymbol{u}}_h, q_h) &= 0 && \forall q_h \in \mathbb{P}^k(\mathcal{T}_h) \end{aligned}}$$

- Optionally, upwind stabilisation can be added through the term

$$\mathrm{j}_h(\underline{\boldsymbol{w}}_h; \underline{\boldsymbol{v}}_h, \underline{\boldsymbol{z}}_h) \coloneqq \sum_{T \in \mathcal{T}_h} \sum_{F \in \mathcal{F}_T} \int_F \frac{\nu}{h_F} \rho(\mathrm{Pe}_{TF}(\boldsymbol{w}_F))(\boldsymbol{v}_F - \boldsymbol{v}_T) \cdot (\boldsymbol{z}_F - \boldsymbol{z}_T)$$

- Weakly enforced boundary conditions can also be considered
- Conservative fluxes can be identified

Well-posedness I

Theorem (Existence and a priori bounds)

There exists a solution $(\underline{\boldsymbol{u}}_h, p_h) \in \underline{\boldsymbol{U}}_{h,0}^k \times P_h^k$ *such that*

$$\|\underline{\boldsymbol{u}}_h\|_{1,h} \lesssim \nu^{-1}\|\boldsymbol{f}\|_{L^2(\Omega)^d}, \text{ and } \|p_h\| \lesssim \left(\|\boldsymbol{f}\|_{L^2(\Omega)^d} + \nu^{-2}\|\boldsymbol{f}\|_{L^2(\Omega)^d}^2\right),$$

with hidden constant independent of both h *and* ν*.*

Theorem (Uniqueness of the discrete solution)

Assume that it holds with C*, independent of* h *and* ν*, small enough,*

$$\|\boldsymbol{f}\|_{L^2(\Omega)^d} \leq C\nu^2.$$

Then, the solution is unique.

Convergence I

Theorem (Convergence to minimal regularity solutions)

It holds up to a subsequence, as $h \to 0$,

- $\boldsymbol{u}_h \to \boldsymbol{u}$ *strongly in* $L^p(\Omega)^d$ *for* $\begin{cases} p \in [1, +\infty) & \text{if } d = 2, \\ p \in [1, 6) & \text{if } d = 3; \end{cases}$
- $\boldsymbol{G}_h^k \underline{\boldsymbol{u}}_h \to \boldsymbol{\nabla} \boldsymbol{u}$ *strongly in* $L^2(\Omega)^{d \times d}$;
- $\mathrm{s}_h(\underline{\boldsymbol{u}}_h, \underline{\boldsymbol{u}}_h) \to 0$;
- $p_h \to p$ *strongly in* $L^2(\Omega)$.

If the exact solution is unique, then the whole sequence converges.

Key tools: Discrete Sobolev embeddings and Rellick–Kondrachov compactness results from [DP and Droniou, 2017a]

Convergence II

Theorem (Convergence rates for small data)

Assume uniqueness for both $(\underline{\boldsymbol{u}}_h, p_h)$ *and* $(\boldsymbol{u}, p)$*. Assume, moreover, the additional regularity* $(\boldsymbol{u}, p) \in H^{k+2}(\Omega)^d \times H^{k+1}(\Omega)$*, as well as*

$$\|\boldsymbol{f}\|_{L^2(\Omega)^d} \leq C\nu^2$$

with C *independent of* h *and* ν *small enough. Then, with hidden constant independent of* h *and* ν*,*

$$\boxed{\|\underline{\boldsymbol{u}}_h - \underline{\boldsymbol{I}}_h^k \boldsymbol{u}\|_{1,h} + \nu^{-1}\|p_h - \pi_h^{0,k} p\|_{L^2(\Omega)} \lesssim h^{k+1} \mathcal{N}_{\boldsymbol{u},p}.}$$

where $\mathcal{N}_{\boldsymbol{u},p} := (1 + \nu^{-1}\|\boldsymbol{u}\|_{H^2(\Omega)^d})\|\boldsymbol{u}\|_{H^{k+2}(\Omega)^d} + \nu^{-1}\|p\|_{H^{k+1}(\Omega)}$.

Static condensation

- Solve the discrete nonlinear problem with a first-order algorithm
- Partition the discrete velocity unknowns as before, and the pressure unknowns into average value + oscillations inside each element
- At each iteration, the linear system has the form

$$\begin{bmatrix} \mathsf{A}_{\mathcal{T}_h\mathcal{T}_h} & \widetilde{\mathsf{B}}_{\mathcal{T}_h} & \mathsf{A}_{\mathcal{T}_h\mathcal{F}_h^{\mathrm{i}}} & \overline{\mathsf{B}}_{\mathcal{T}_h} \\ \mathsf{A}_{\mathcal{F}_h^{\mathrm{i}}\mathcal{T}_h} & \widetilde{\mathsf{B}}_{\mathcal{F}_h^{\mathrm{i}}} & \mathsf{A}_{\mathcal{F}_h^{\mathrm{i}}\mathcal{F}_h^{\mathrm{i}}} & \overline{\mathsf{B}}_{\mathcal{F}_h^{\mathrm{i}}} \\ \widetilde{\mathsf{B}}_{\mathcal{T}_h}^{\mathrm{T}} & 0 & \widetilde{\mathsf{B}}_{\mathcal{F}_h^{\mathrm{i}}}^{\mathrm{T}} & 0 \\ \overline{\mathsf{B}}_{\mathcal{T}_h}^{\mathrm{T}} & 0 & \overline{\mathsf{B}}_{\mathcal{F}_h^{\mathrm{i}}}^{\mathrm{T}} & 0 \end{bmatrix} \begin{bmatrix} \mathsf{U}_{\mathcal{T}_h} \\ \widetilde{\mathsf{P}}_{\mathcal{T}_h} \\ \mathsf{U}_{\mathcal{F}_h^{\mathrm{i}}} \\ \overline{\mathsf{P}}_{\mathcal{T}_h} \end{bmatrix} = \begin{bmatrix} \mathsf{F}_{\mathcal{T}_h} \\ 0 \\ 0 \\ 0 \end{bmatrix}$$

- Static condensation of $\mathsf{U}_{\mathcal{T}_h}$ and $\widetilde{\mathsf{P}}_{\mathcal{T}_h}$ is possible

Convergence rate: Kovasznay flow

- Following [Kovasznay, 1948], let $\Omega \coloneqq (-0.5, 1.5) \times (0, 2)$ and set

$$\mathrm{Re} \coloneqq (2\nu)^{-1}, \qquad \lambda \coloneqq \mathrm{Re} - \left(\mathrm{Re}^2 + 4\pi^2\right)^{\frac{1}{2}}$$

- The components of the velocity are given by

$$u_1(\boldsymbol{x}) \coloneqq 1 - \exp(\lambda x_1)\cos(2\pi x_2), \qquad u_2(\boldsymbol{x}) \coloneqq \frac{\lambda}{2\pi}\exp(\lambda x_1)\sin(2\pi x_2),$$

  and pressure given by

$$p(\boldsymbol{x}) \coloneqq -\frac{1}{2}\exp(2\lambda x_1) + \frac{\lambda}{2}\left(\exp(4\lambda) - 1\right)$$

- We monitor the errors

$$\boxed{\underline{\boldsymbol{e}}_h \coloneqq \underline{\boldsymbol{u}}_h - \underline{\boldsymbol{I}}_h^k \boldsymbol{u}, \qquad \epsilon_h \coloneqq p_h - \pi_h^{0,k} p}$$

Convergence rate: Kovasznay flow

Strongly enforced BC, upwind stabilisation, $\mathrm{Re} = 40$

N_{dof}	N_{nz}	$\|\underline{\boldsymbol{e}}_{\boldsymbol{h}}\|_{\boldsymbol{\nu},h}$	EOC	$\|\boldsymbol{e}_{\boldsymbol{h}}\|_{\boldsymbol{L}^2(\Omega)\boldsymbol{d}}$	EOC	$\|\epsilon_{\boldsymbol{h}}\|_{\boldsymbol{L}^2(\Omega)}$	EOC	τ_{ass}	τ_{sol}
				$k = 0$					
65	736	9.37e-01	–	1.40e-01	–	6.84e-01	–	1.31e-02	8.52e-03
289	3808	1.13e+00	-0.27	5.50e-01	-1.98	1.96e-01	1.80	5.92e-02	4.90e-02
1217	17056	9.14e-01	0.31	2.26e-01	1.28	1.02e-01	0.94	1.02e-01	1.06e-01
4993	71968	6.26e-01	0.55	7.89e-02	1.52	3.52e-02	1.54	3.10e-01	4.46e-01
20225	295456	3.87e-01	0.70	2.47e-02	1.68	9.78e-03	1.85	1.02e+00	2.17e+00
81409	1197088	2.47e-01	0.65	8.06e-03	1.61	3.09e-03	1.66	3.73e+00	1.49e+01
				$k = 1$					
113	2464	7.31e-01	–	5.37e-01	–	2.49e-01	–	2.51e-02	1.72e-02
513	13056	3.83e-01	0.93	1.54e-01	1.80	4.29e-02	2.54	4.77e-02	4.72e-02
2177	59008	1.02e-01	1.90	2.13e-02	2.85	3.98e-03	3.43	1.29e-01	1.79e-01
8961	249984	2.93e-02	1.80	2.97e-03	2.84	6.54e-04	2.61	5.13e-01	1.01e+00
36353	1028224	8.23e-03	1.83	3.99e-04	2.90	1.28e-04	2.35	2.05e+00	5.28e+00
146433	4169856	2.26e-03	1.86	5.21e-05	2.94	2.65e-05	2.27	7.25e+00	2.97e+01
				$k = 2$					
161	5216	3.50e-01	–	2.09e-01	–	6.42e-02	–	3.44e-02	2.26e-02
737	27872	3.76e-02	3.22	1.34e-02	3.96	2.07e-03	4.95	6.95e-02	6.88e-02
3137	126368	6.96e-03	2.43	1.31e-03	3.36	1.48e-04	3.80	2.66e-01	3.60e-01
12929	536096	1.06e-03	2.72	9.48e-05	3.79	1.77e-05	3.07	1.11e+00	2.02e+00
52481	2206496	1.55e-04	2.77	6.36e-06	3.90	2.27e-06	2.96	4.16e+00	1.13e+01
211457	8951072	2.21e-05	2.81	4.13e-07	3.95	2.72e-07	3.06	1.51e+01	6.02e+01
				$k = 5$					
305	19616	2.28e-03	–	1.05e-03	–	1.70e-04	–	1.28e-01	5.63e-02
1409	105728	4.01e-05	5.83	1.05e-05	6.65	2.05e-06	6.37	3.95e-01	2.19e-01
6017	480896	7.21e-07	5.80	8.98e-08	6.87	3.21e-08	6.00	1.60e+00	1.32e+00
24833	2043008	1.37e-08	5.72	7.89e-10	6.83	5.43e-10	5.88	6.45e+00	8.29e+00
100865	8414336	2.56e-10	5.74	6.72e-12	6.88	9.14e-12	5.89	2.54e+01	5.01e+01

Convergence rate: Kovasznay flow

Weakly enforced BC, no stabilisation, $\mathrm{Re} = 40$

N_{dof}	N_{nz}	$\|\underline{\boldsymbol{e}}_{\boldsymbol{h}}\|_{\boldsymbol{\nu},h}$	EOC	$\|\boldsymbol{e}_{\boldsymbol{h}}\|_{\boldsymbol{L}^2(\Omega)^d}$	EOC	$\|\epsilon_{\boldsymbol{h}}\|_{\boldsymbol{L}^2(\Omega)}$	EOC	τ_{ass}	τ_{sol}
				$k = 0$					
97	1216	1.07e+00	–	3.93e-01	–	6.80e-01	–	2.68e-02	2.31e-02
353	4800	1.70e+00	-0.67	9.58e-01	-1.28	2.79e-01	1.28	3.41e-02	3.71e-02
1345	19072	1.44e+00	0.24	3.89e-01	1.30	1.32e-01	1.09	6.68e-02	8.04e-02
5249	76032	8.77e-01	0.72	1.18e-01	1.72	4.93e-02	1.42	2.15e-01	3.52e-01
20737	303616	4.78e-01	0.88	3.23e-02	1.87	1.49e-02	1.72	8.07e-01	1.95e+00
82433	1213440	2.46e-01	0.96	8.32e-03	1.96	4.08e-03	1.87	3.19e+00	1.47e+01
				$k = 1$					
177	4256	1.02e+00	–	7.27e-01	–	2.69e-01	–	1.44e-02	1.60e-02
641	16768	4.20e-01	1.28	1.66e-01	2.13	4.96e-02	2.44	3.59e-02	4.25e-02
2433	66560	1.40e-01	1.58	2.66e-02	2.64	8.60e-03	2.53	1.09e-01	1.70e-01
9473	265216	4.06e-02	1.79	3.55e-03	2.91	1.29e-03	2.74	4.62e-01	1.10e+00
37377	1058816	1.03e-02	1.97	4.37e-04	3.02	1.79e-04	2.85	1.91e+00	5.64e+00
148481	4231168	2.61e-03	1.99	5.46e-05	3.00	2.96e-05	2.60	7.07e+00	3.32e+01
				$k = 2$					
257	9152	5.50e-01	–	3.16e-01	–	1.20e-01	–	2.23e-02	2.33e-02
929	36032	7.58e-02	2.86	2.46e-02	3.68	6.03e-03	4.31	6.11e-02	7.47e-02
3521	142976	1.23e-02	2.62	1.84e-03	3.74	3.69e-04	4.03	2.41e-01	3.90e-01
13697	569600	1.70e-03	2.86	1.12e-04	4.03	3.63e-05	3.35	1.02e+00	2.21e+00
54017	2273792	2.21e-04	2.95	6.87e-06	4.03	3.84e-06	3.24	3.62e+00	1.17e+01
214529	9085952	2.80e-05	2.98	4.28e-07	4.00	3.72e-07	3.37	1.40e+01	6.76e+01
				$k = 5$					
497	34976	6.48e-03	–	1.76e-03	–	1.02e-03	–	1.23e-01	7.22e-02
1793	137600	7.07e-05	6.52	1.34e-05	7.04	4.58e-06	7.81	4.06e-01	2.95e-01
6785	545792	1.28e-06	5.79	1.10e-07	6.94	4.40e-08	6.70	1.51e+00	1.56e+00
26369	2173952	2.20e-08	5.87	8.84e-10	6.95	5.86e-10	6.23	5.67e+00	8.48e+00
103937	8677376	3.56e-10	5.95	7.20e-12	6.94	7.42e-12	6.30	2.28e+01	5.14e+01

Lid-driven cavity I

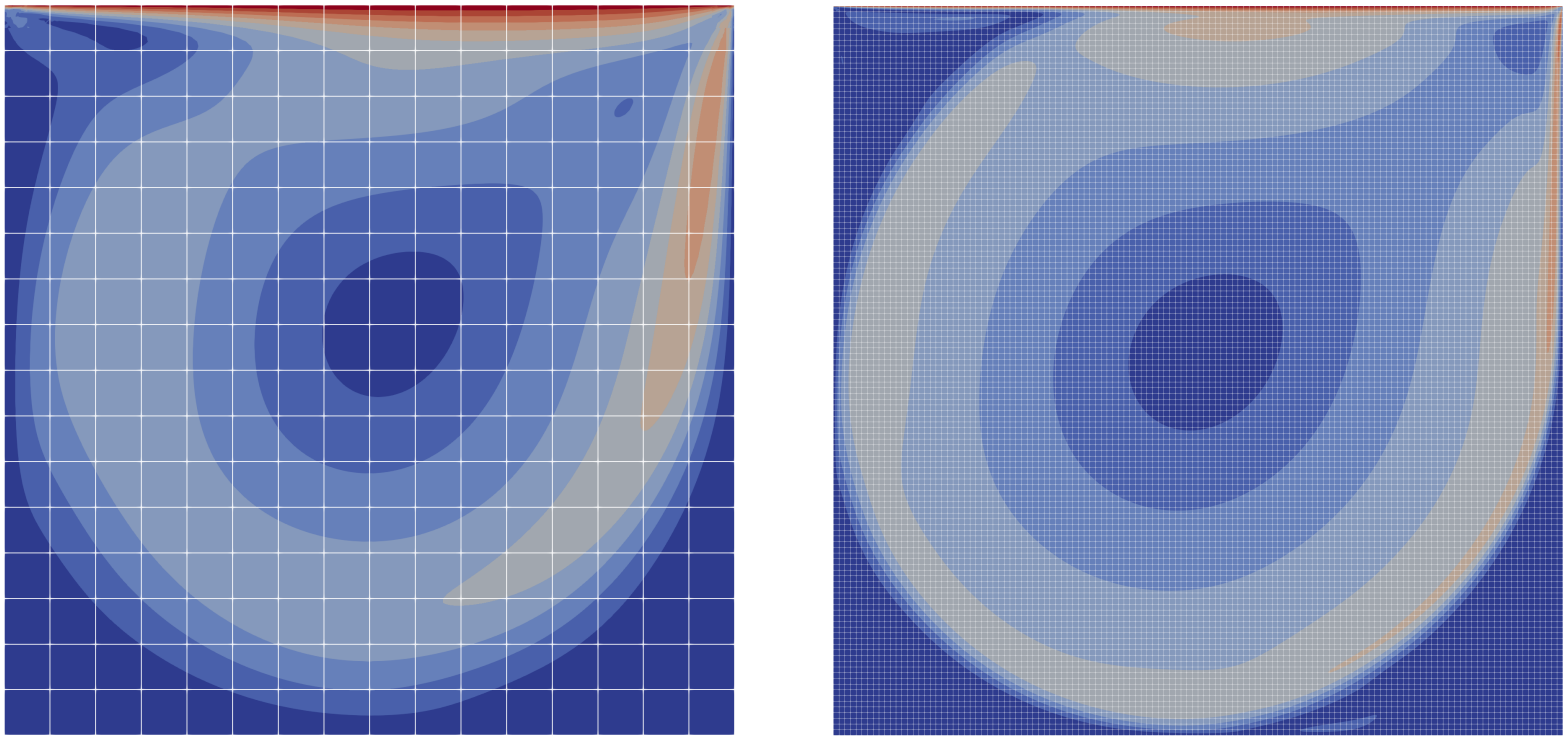

Figure: Lid-driven cavity, velocity magnitude contours (10 equispaced values in the range $[0, 1]$) for $k = 7$ computations at $\mathrm{Re} = 1{,}000$ (*left*: 16x16 grid) and $\mathrm{Re} = 20{,}000$ (*right*: 128x128 grid).

Lid-driven cavity

Re = 1,000

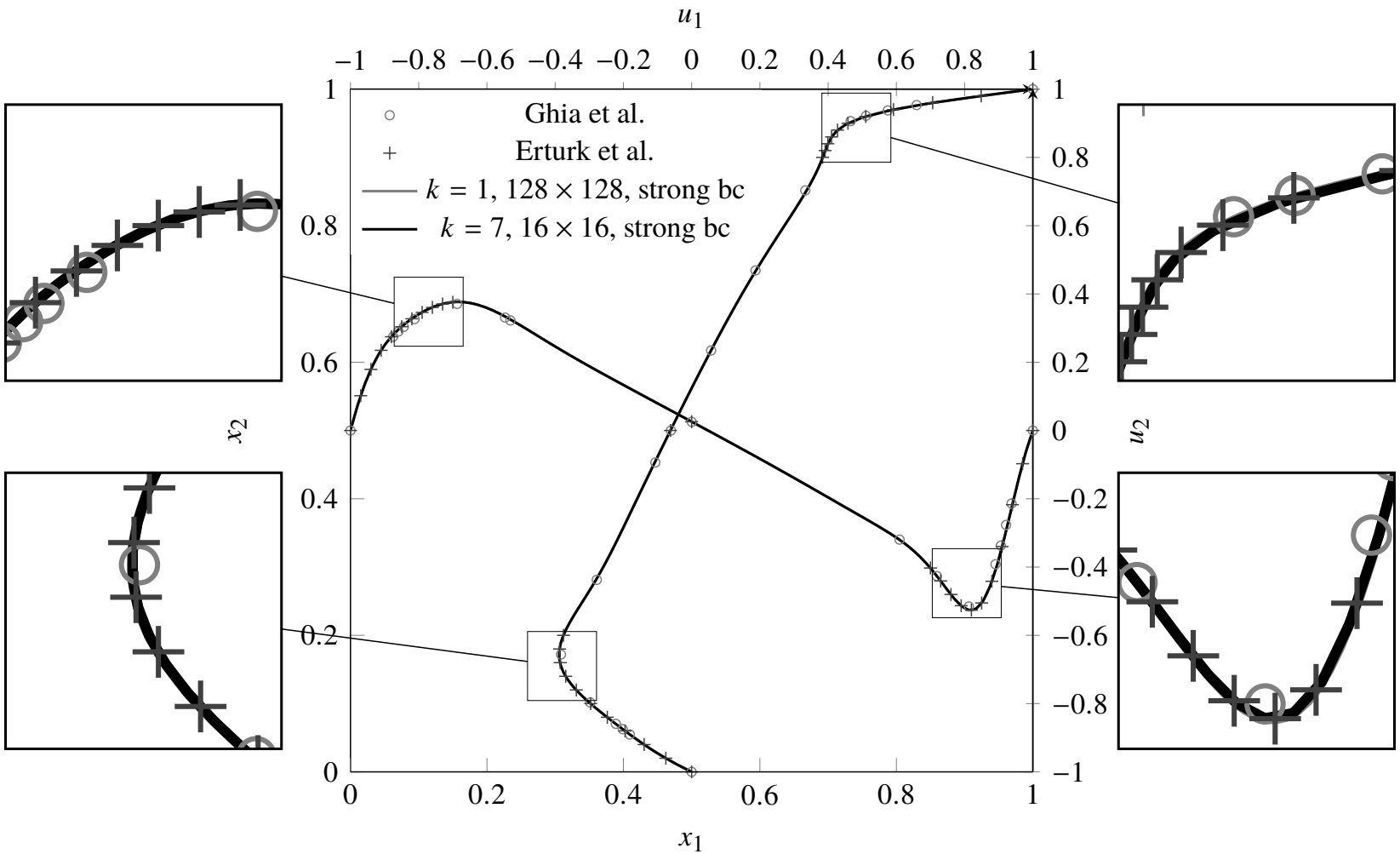

Figure: u_1 along the vertical centerline, u_2 along the horizontal centerline

Lid-driven cavity

Re = 5,000

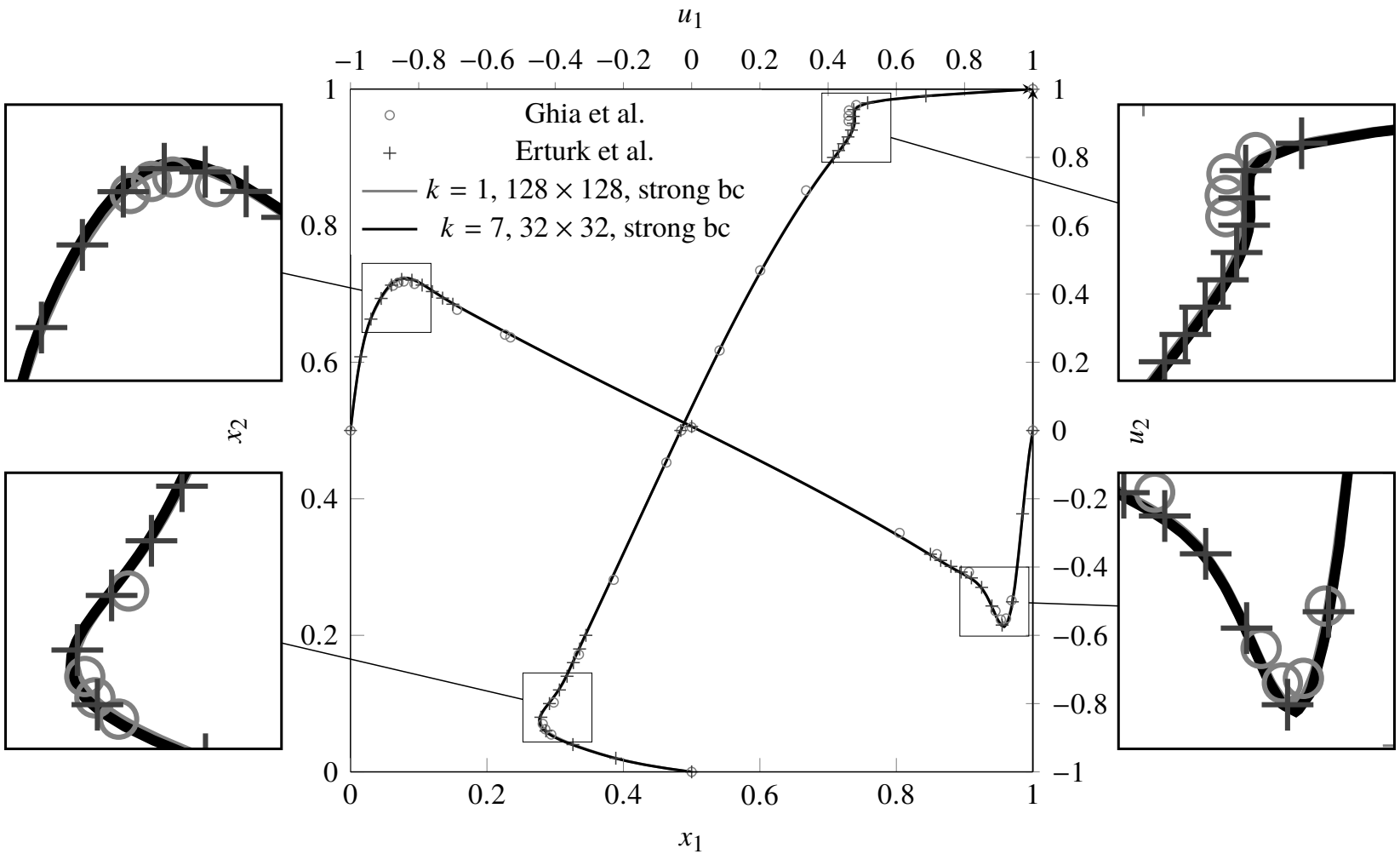

Figure: u_1 along the vertical centerline, u_2 along the horizontal centerline

Lid-driven cavity

Re = 10,000

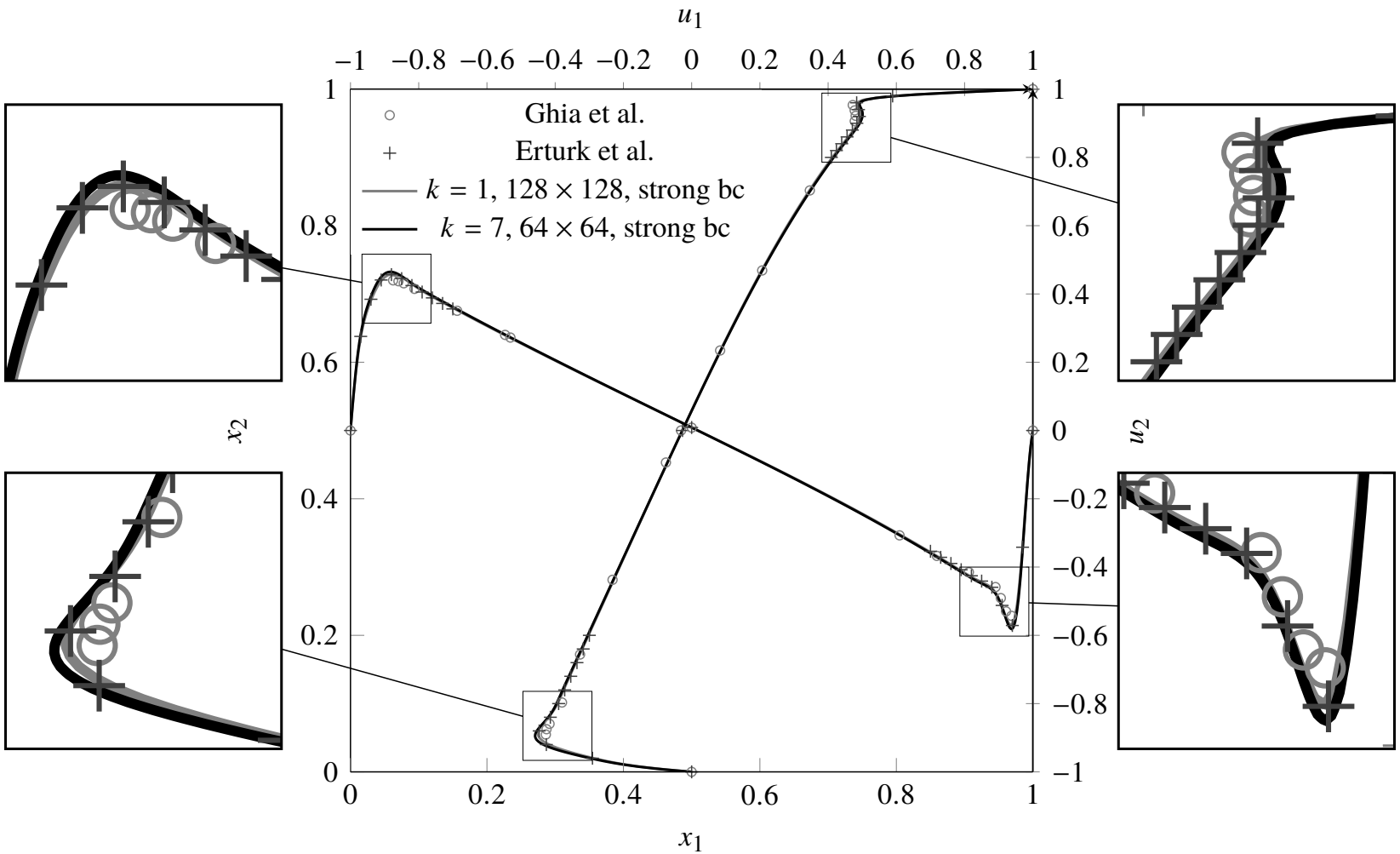

Figure: u_1 along the vertical centerline, u_2 along the horizontal centerline

Lid-driven cavity

Re = 20,000

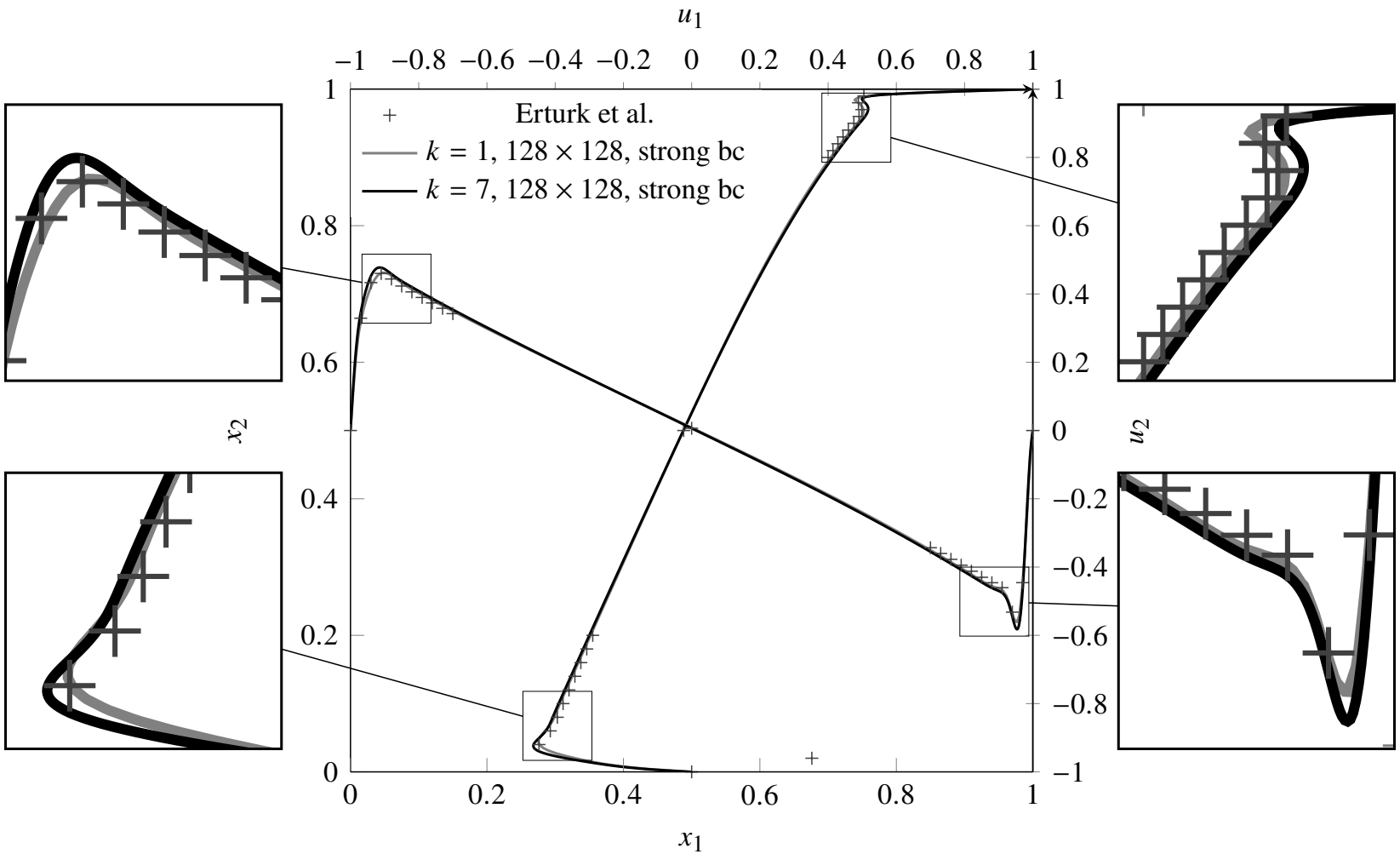

Figure: u_1 along the vertical centerline, u_2 along the horizontal centerline

Three-dimensional lid-driven cavity

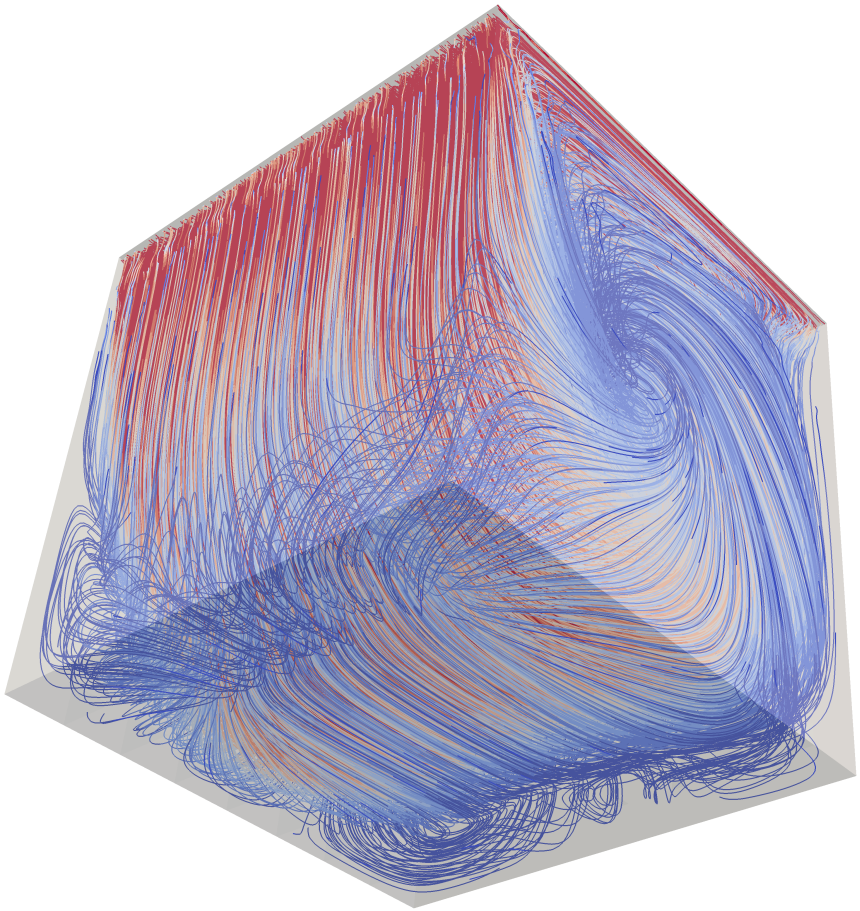

Figure: Three-dimensional lid-driven cavity, $\mathrm{Re} = 1000$, streamlines

Lid-driven cavity

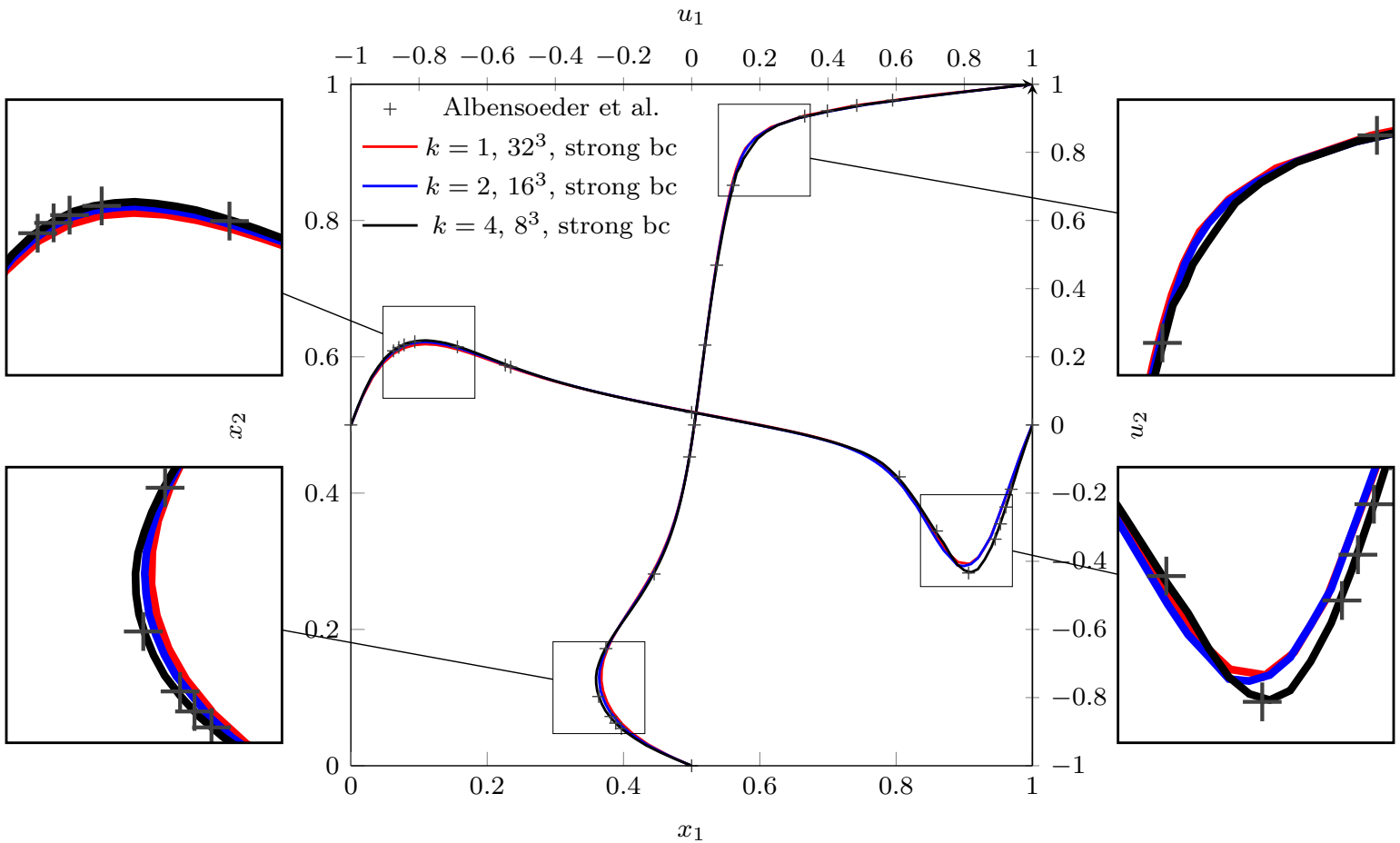

Figure: 3D Lid-driven cavity flow, horizontal component u_1 of the velocity along the vertical centerline $x_1, x_3 = \frac{1}{2}$ and the vertical component u_2 of the velocity along the horizontal centerline $x_2, x_3 = \frac{1}{2}$ for $\mathrm{Re} = 1{,}000$, $k = 1, 2, 4$

Lid-driven cavity

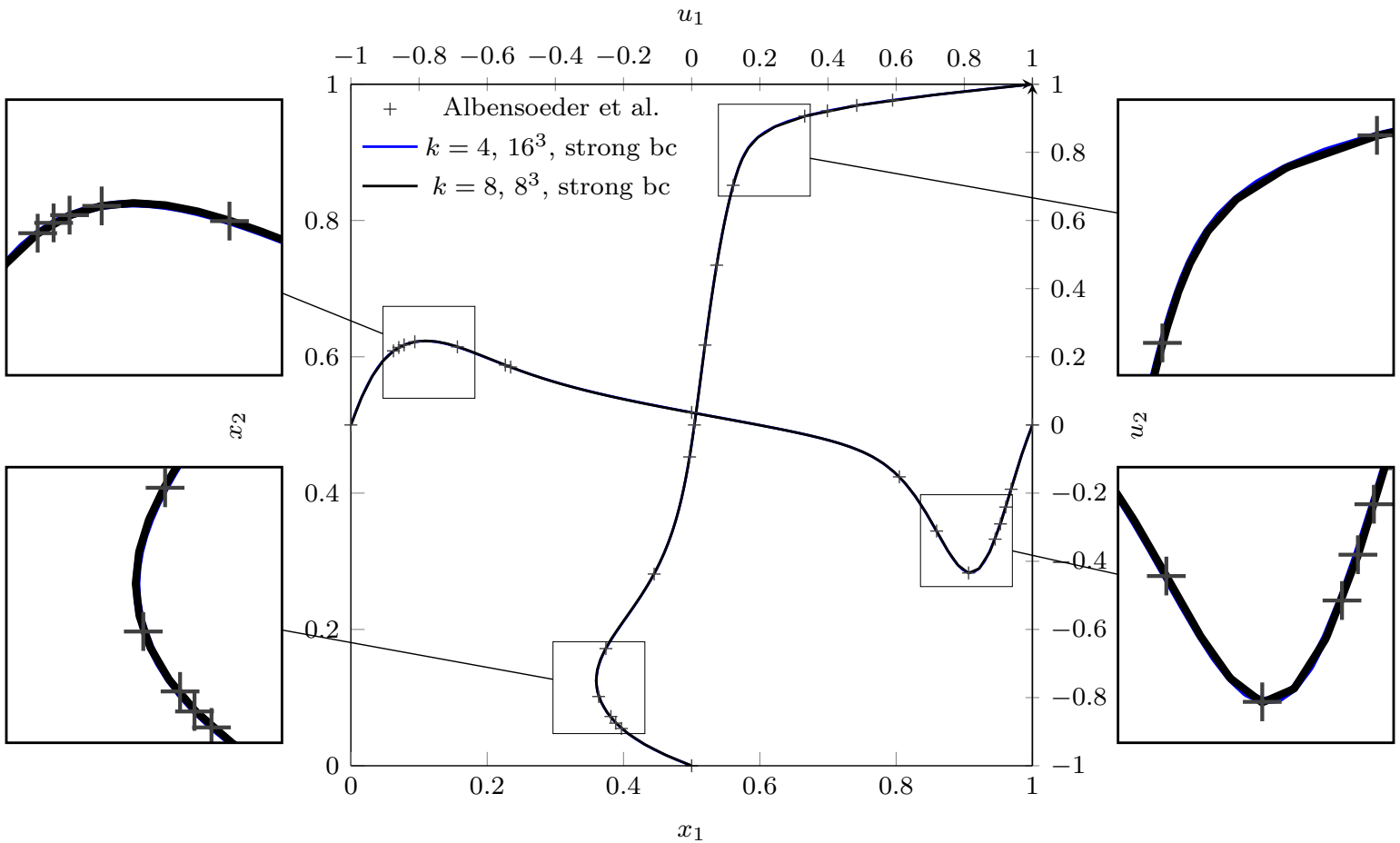

Figure: 3D Lid-driven cavity flow, horizontal component u_1 of the velocity along the vertical centerline $x_1, x_3 = \frac{1}{2}$ and the vertical component u_2 of the velocity along the horizontal centerline $x_2, x_3 = \frac{1}{2}$ for $\mathrm{Re} = 1{,}000$, $k = 4, 8$

Thank you for your attention!

Coming soon:

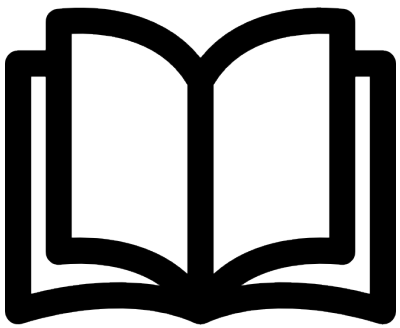

D. A. Di Pietro and J. Droniou

The Hybrid High-Order Method for Polytopal Meshes

Design, Analysis and Applications

References I

Aghili, J., Boyaval, S., and Di Pietro, D. A. (2015).

Hybridization of mixed high-order methods on general meshes and application to the Stokes equations.
Comput. Meth. Appl. Math., 15(2):111–134.

Aghili, J. and Di Pietro, D. A. (2018).

An advection-robust Hybrid High-Order method for the Oseen problem.
J. Sci. Comput.
Published online.

Botti, L., Di Pietro, D. A., and Droniou, J. (2018).

A Hybrid High-Order discretisation of the Brinkman problem robust in the Darcy and Stokes limits.
Comput. Meth. Appl. Mech. Engrg., 341:278–310.

Botti, L., Di Pietro, D. A., and Droniou, J. (2019).

A Hybrid High-Order method for the incompressible Navier–Stokes equations based on Temam's device.
J. Comput. Phys., 376:786–816.

Di Pietro, D. A. and Droniou, J. (2017a).

A Hybrid High-Order method for Leray–Lions elliptic equations on general meshes.
Math. Comp., 86(307):2159–2191.

Di Pietro, D. A. and Droniou, J. (2017b).

$W^{s,p}$-approximation properties of elliptic projectors on polynomial spaces, with application to the error analysis of a Hybrid High-Order discretisation of Leray–Lions problems.
Math. Models Methods Appl. Sci., 27(5):879–908.

Di Pietro, D. A. and Ern, A. (2015).

A hybrid high-order locking-free method for linear elasticity on general meshes.
Comput. Methods Appl. Mech. Engrg., 283:1–21.

References II

Di Pietro, D. A., Ern, A., Linke, A., and Schieweck, F. (2016).

A discontinuous skeletal method for the viscosity-dependent Stokes problem.
Comput. Meth. Appl. Mech. Engrg., 306:175–195.

Di Pietro, D. A. and Krell, S. (2018).

A Hybrid High-Order method for the steady incompressible Navier–Stokes problem.
J. Sci. Comput., 74(3):1677–1705.

Di Pietro, D. A. and Specogna, R. (2016).

An a posteriori-driven adaptive Mixed High-Order method with application to electrostatics.
J. Comput. Phys., 326(1):35–55.

Di Pietro, D. A. and Tittarelli, R. (2018).

Numerical Methods for PDEs, chapter An introduction to Hybrid High-Order methods.
Number 15 in SEMA-SIMAI. Springer.

Kovasznay, L. S. G. (1948).

Laminar flow behind a two-dimensional grid.
Proc. Camb. Philos. Soc., 44:58–62.

Temam, R. (1979).

Navier-Stokes equations, volume 2 of *Studies in Mathematics and its Applications*.
North-Holland Publishing Co., Amsterdam-New York, revised edition.
Theory and numerical analysis, With an appendix by F. Thomasset.